# Leptonic neutral-current probes in a short-distance DUNE-like setup

Salvador Centelles Chuliá [1,*] O. G. Miranda [2,†] and Jose W. F. Valle [3,‡]

[1] *Max-Planck-Institut für Kernphysik, Saupfercheckweg 1, 69117 Heidelberg, Germany*
[2] *Departamento de Física, Centro de Investigación y de Estudios, Avanzados del IPN Apdo. Postal 14-740 07000 Ciudad de México, Mexico*
[3] *AHEP Group, Institut de Física Corpuscular—CSIC/Universitat de València, Parc Científic de Paterna. C/ Catedrático José Beltrán, 2 E-46980 Paterna, Valencia, Spain*

(Received 8 February 2024; accepted 30 April 2024; published 7 June 2024)

Precision measurements of neutrino-electron scattering may provide a viable way to test the nonminimal form of the charged and neutral current weak interactions within a hypothetical near-detector setup for the Deep Underground Neutrino Experiment (DUNE). Although low-statistics, these processes are clean and provide information complementing the results derived from oscillation studies. They could shed light on the scale of neutrino mass generation in low-scale seesaw schemes.

DOI: 10.1103/PhysRevD.109.115007

## I. INTRODUCTION

Ever since the historic discovery of neutrino oscillations [1,2] indicating the need for neutrino masses, most progress in neutrino physics has relied on experiments involving charged current (CC) processes. However, the observation of coherent elastic neutrino-nucleus scattering (CEvNS) [3,4] proposed long ago in the pioneer papers [5,6], has prompted a neutral current (NC) revival and the recognition that the NC can provide an interesting and complementary way to study neutrinos.

Moreover, it has long been known from theory that, if neutrino mass generation is mediated by heavy neutrino exchange, the structure of both the CC and NC is nontrivial [7,8]. Indeed, the mixing matrix, $K$, characterizing the leptonic CC weak interaction that describes oscillations is not unitary, while the NC interaction of mass-eigenstate neutrinos involves a matrix $P$ that deviates from the unit matrix. Moreover, these two matrices are related [7,8].

Although the effect of nonunitary neutrino mixing was first discussed in the context of astrophysical neutrino propagation [9–11], it can be phenomenologically relevant in Earth-bound experiments. This happens in the context of genuine low-scale seesaw schemes, such as the inverse [12,13] or the linear seesaw mechanism [14–16], leading to potentially sizeable deviations from the conventional leptonic weak currents with unitary CC mixing. These corrections are expressed as power series in the parameter $\varepsilon = \mathcal{O}(Yv/M)$, where $M$ is the mediator mass scale and $v$ is the standard model (SM) vacuum expectation value (VEV). Although small, we stress that $\varepsilon$ can be non-negligible within low-scale realizations of the seesaw. The effects of unitarity violation and the new associated neutrino phenomena have been extensively explored in the recent literature, mainly devoted to charged-current processes on hadronic probes [17–42].

Here we explore the potential of leptonic probes such as the scattering process $\nu + e^- \to \nu + e^-$ as a potentially viable way to test the nonminimal form of the CC and NC weak interactions. This has already been discussed in [43,44] in the context of hadronic probes. In this paper we speculate that leptonic probes, too, may be useful within a DUNE-like near-detector setup. Although they have low-statistics, these processes are clean and provide information complementing the results derived from oscillation studies [45], shedding light on the scale of neutrino mass generation within low-scale seesaw schemes.

## II. THEORY PRELIMINARIES

The most general CC weak interaction of massive neutrinos is described by a rectangular matrix $K$ [7]. A short summary of the main features and notation is as follows. In the basis where the charged lepton mass matrix is diagonal, the upper blocks are simply the first three rows of the neutrino mixing matrix [8]. We can also define the relevant sub-block as

$$K = (\, N \quad S \,). \tag{1}$$

[*] chulia@mpi-hd.mpg.de
[†] omar.miranda@cinvestav.mx
[‡] valle@ific.uv.es

With three active neutrino flavors, $N$ is a $3\times3$ matrix, while $S$ is a $3\times m$ matrix, with $m$ the number of fermionic singlets that mix with the active neutrinos.[1] The small block $S\sim\mathcal{O}(\varepsilon)$ is the seesaw expansion matrix [8]. Notice that $KK^\dagger=I_{3\times3}$ and therefore $NN^\dagger=1-SS^\dagger\sim1-\mathcal{O}(\varepsilon^2)$. On the other hand, the matrix $P$ describing the NC-neutrino interactions [7] is given by

$$P=K^\dagger K\neq I. \tag{2}$$

If the energy of a given process is much lower than the masses of the heavy mediators these will not be produced. For example, the heavy states will not take part in oscillation experiments. Then, effectively, only the first $3\times3$ blocks of $K$ and $P$ will play a role in the weak interactions, i.e., $N$ in the charged current and $N^\dagger N$ in the neutral current. This would signal the presence of unitarity violation in the neutrino mixing matrix [9] whose general description is given in [17]. A systematic approach to the (nonunitary) matrix $N$ can be derived from the seesaw expansion [8], as the lower-triangular parametrization proposed in [17],[2]

$$N=\begin{pmatrix}\alpha_{11} & 0 & 0\\ \alpha_{21} & \alpha_{22} & 0\\ \alpha_{31} & \alpha_{31} & \alpha_{33}\end{pmatrix}\cdot U. \tag{3}$$

Besides the $3\times3$ unitary matrix $U$ used to describe neutrino mixing in the conventional unitary case, one has the triangular prefactor characterized by three diagonal $\alpha_{ii}$ ($i=1$, 2, 3), real and close to 1, and three nondiagonal $\alpha_{ij}$ ($i\neq j$) which are small but complex. This is a convenient and complete description of nonunitarity. By construction, $N$ and $S$ must satisfy the relation $NN^\dagger=1-SS^\dagger$, hence $NN^\dagger\sim1-\mathcal{O}(\varepsilon^2)$. Explicitly,

$$NN^\dagger=\begin{pmatrix}\alpha_{11}^2 & \alpha_{11}\alpha_{21}^* & \alpha_{11}\alpha_{31}^*\\ \alpha_{11}\alpha_{21} & \alpha_{22}^2+|\alpha_{21}|^2 & \alpha_{22}\alpha_{32}^*+\alpha_{21}\alpha_{31}^*\\ \alpha_{11}\alpha_{31} & \alpha_{22}\alpha_{32}+\alpha_{21}^*\alpha_{31} & \alpha_{33}^2+|\alpha_{31}|^2+|\alpha_{32}|^2\end{pmatrix}, \tag{4}$$

from where one can read off the strength of the $\alpha_{ij}$ in terms of the small seesaw expansion parameter $\varepsilon$. Indeed, within the seesaw paradigm, the leading deviation from the standard form of the CC mixing matrix lies in the diagonal entries $NN^\dagger\sim1-\mathcal{O}(\varepsilon^2)$ implying that, for example, $\alpha_{11}^2\sim1-\mathcal{O}(\varepsilon^2)$. Hence, $\alpha_{11}\alpha_{21}\sim\mathcal{O}(\varepsilon^2)$, so that $\alpha_{21}\sim\mathcal{O}(\varepsilon^2)$ and

$$\alpha_{ii}^2\sim1-\mathcal{O}(\varepsilon^2), \tag{5}$$

$$|\alpha_{ij}|^2\sim\mathcal{O}(\varepsilon^4),\qquad i\neq j. \tag{6}$$

One sees that the strength of the off-diagonal $\alpha$'s is suppressed relative to the deviations of the flavor-diagonal ones from their SM values. In other words, in the seesaw expansion the zeroth order corresponds to the unitary limit, the first order gives only diagonal flavor-conserving effects, while the genuine flavor-violating effects nonunitary corrections only come at second order. Notice also that this behavior is consistent with the validity of the well-known triangle inequality $|\alpha_{ij}|\leq\sqrt{(1-\alpha_{ii}^2)(1-\alpha_{jj}^2)}$ [17].

Additionally, it is important to notice that unitarity violation leads to a redefinition of the Fermi constant, extracted from the $\mu^-$ lifetime assuming the SM. In the presence of nonunitarity the measured quantity would be the effective muon decay coupling $G_\mu$. Since the $W$-boson vertices are modified by the nonunitarity parameters one finds

$$G_\mu=1.1663787(6)\times10^{-5}\ \mathrm{GeV}^{-2}\quad(\text{effective }\mu^-\text{ decay constant, [47]}), \tag{7}$$

$$G_\mu^2=G_F^2(NN^\dagger)_{ee}(NN^\dagger)_{\mu\mu}, \tag{8}$$

and therefore,

$$1\leq\frac{G_F^2}{G_\mu^2}=\frac{1}{(NN^\dagger)_{ee}(NN^\dagger)_{\mu\mu}}\approx3-\alpha_{11}^2-\alpha_{22}^2\sim1+\mathcal{O}(\varepsilon^2). \tag{9}$$

Therefore, in the presence of nonunitarity any process proportional to $G_F^2$ will get an "enhancement". This is counterintuitive, because naively one expects less events than in the SM if the mixing is nonunitary, due to kinematically inaccessible heavy states. The reduction of the event number due to nonunitarity and the "increase" due to the redefinition of $G_F$ compete with each other, so that in some cases one can achieve $\mathcal{N}_{\mathrm{NU}}/\mathcal{N}_{\mathrm{U}}=1$ even in the presence of nonunitarity.

## III. $\nu_\mu-e^-$ SCATTERING IN THE PRESENCE OF NONUNITARITY AT ZERO DISTANCE

We now turn our attention to the scattering of a muon neutrino on an electron target in the presence of nonunitarity. The relevant Feynman diagrams, given in Figs. 1 and 2, describe the elastic electron-neutrino scattering

[1]In the most general SM-seesaw one can have any number of "right-handed" neutrino mediators, since they are gauge singlets [7].

[2]An alternative description and its relationship with Eq. (3) is discussed in Ref. [46].

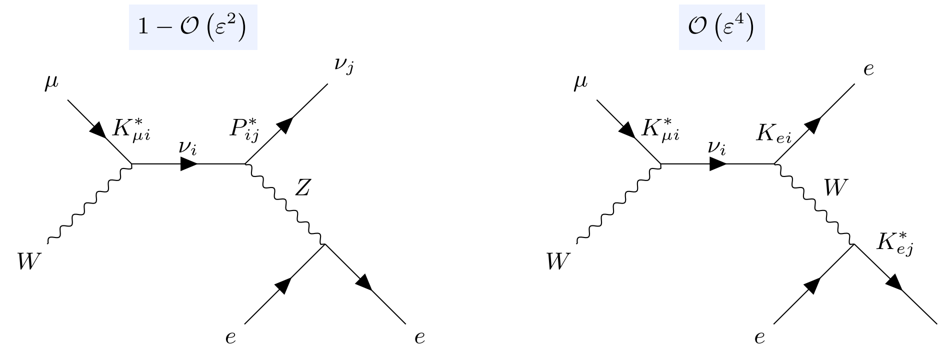


FIG. 1. Feynman diagrams for $\nu_\mu + e^-$ scattering, where the $\nu_\mu$ is produced via the usual CC vertex, while the final-state detection involves the NC (left diagram), with a subleading CC contribution of order $\varepsilon^4$ (right diagram).

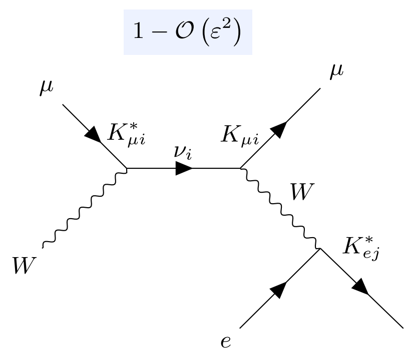


FIG. 2. Feynman diagram for the charged current process $\nu_\mu + e^- \to \nu + \mu^-$ in the nonunitary case.

and the neutrino-induced muon production processes, respectively.

### A. Neutrino-electron elastic scattering

At tree level the two relevant diagrams are given in Fig. 1. The vertex on the left of each diagram corresponds to CC $\nu_\mu$ production, while the vertex on the right depicts either the NC and CC detection modes, respectively. Within the three neutrino paradigm, with unitary lepton mixing, the CC channel (right panel of Fig. 1) does not contribute at zero distance. In such case, the process is pure NC (left panel of Fig. 1) and the differential cross section is given by

$$\left(\frac{d\sigma}{dT}\right)^{\mathrm{SM}} = \frac{2G_\mu^2 m_e}{\pi}\left(g_L^2 + g_R^2\left(1-\frac{T}{E\nu}\right)^2 - g_L g_R \frac{m_e T}{E_\nu^2}\right), \tag{10}$$

where $g_L = -1/2 + \sin^2\theta_{\mathrm{W}}$ and $g_R = -\sin^2\theta_{\mathrm{W}}$. However, in the presence of nonunitarity the CC contribution is in general nonzero. In this case, the cross section is replaced by

$$\begin{aligned}\left(\frac{d\sigma}{dT}\right)^{\mathrm{NU}} &= \frac{\mathcal{P}^{\mathrm{NC}}_{\mu e}}{(NN^\dagger)_{ee}(NN^\dagger)_{\mu\mu}}\left(\frac{d\sigma}{dT}\right)^{\mathrm{SM}} \\ &\quad + \frac{2m_e G_\mu^2}{\pi}\frac{\mathcal{R}e[\mathcal{P}^{\mathrm{int}}_{\mu e}]}{(NN^\dagger)_{ee}(NN^\dagger)_{\mu\mu}} \\ &\quad \times\left\{\frac{\mathcal{P}^{\mathrm{CC}}_{\mu e}}{\mathcal{R}e[\mathcal{P}^{\mathrm{int}}_{\mu e}]} + 2g_L - g_R\frac{m_e T}{E_\nu^2}\right\}, \end{aligned} \tag{11}$$

where the probability factors are given by

$$\mathcal{P}^{\mathrm{NC}}_{\mu e} = (NN^\dagger NN^\dagger NN^\dagger)_{\mu\mu}, \tag{12}$$

$$\mathcal{P}^{\mathrm{CC}}_{\mu e} = (NN^\dagger)_{\mu e}(NN^\dagger)_{e\mu}(NN^\dagger)_{ee}, \tag{13}$$

$$\mathcal{P}^{\mathrm{int}}_{\mu e} = (NN^\dagger NN^\dagger)_{e\mu}(NN^\dagger)_{\mu e}. \tag{14}$$

Note that, in general, the slope of the differential cross section in the presence of nonunitarity differs from that expected in the SM, as it changes the relative weight between the $T$-dependent and constant terms. This is determined by the actual values of the probability factors, in turn specified by the nonunitarity parameters $\alpha_{ij}$. While the exact expression in Eq. (11) is a complicated function of the $\alpha_{ij}$, one can write it in powers of the seesaw expansion parameter $\varepsilon$ by following the prescription given in Eqs. (5) and (6). This implies that, to $\mathcal{O}(\varepsilon^2)$, the SM kinematic structure is preserved, and one has just an overall rescaling compared to the SM expectation,

$$\left(\frac{d\sigma}{dT}\right)^{\mathrm{NU}} \approx (2\alpha_{22}^2 - \alpha_{11}^2)\left(\frac{d\sigma}{dT}\right)^{\mathrm{SM}} + \mathcal{O}(\varepsilon^4). \tag{15}$$

This can be understood by expanding the NC probability factor in powers of $\varepsilon$ and noticing that the leading term is of order $1-\mathcal{O}(\varepsilon^2)$ and can be written as

$$\mathcal{P}^{\mathrm{NC}}_{\mu e} = (NN^\dagger NN^\dagger NN^\dagger)_{\mu\mu} \approx 3\alpha_{22}^2 - 2 \sim 1 - \mathcal{O}(\varepsilon^2), \tag{16}$$

while the CC and interference probability factors are instead $\mathcal{O}(\varepsilon^4)$, i.e.,

$$\mathcal{P}_{\mu e}^{\mathrm{CC}} = (NN^\dagger)_{\mu e}(NN^\dagger)_{e\mu}(NN^\dagger)_{ee} = \alpha_{11}^4|\alpha_{21}|^2 \sim \mathcal{O}(\varepsilon^4), \tag{17}$$

$$\mathcal{P}_{\mu e}^{\mathrm{int}} = (NN^\dagger NN^\dagger)_{e\mu}(NN^\dagger)_{\mu e} \approx 2|\alpha_{21}|^2 \sim \mathcal{O}(\varepsilon^4). \tag{18}$$

Therefore, up to $\mathcal{O}(\varepsilon^2)$ terms one can neglect the CC and interference contributions, hence recovering the same kinematic structure characteristic of the SM and given by Eq. (10). Deviations from the SM kinematic structure come only at order $\mathcal{O}(\varepsilon^4)$, due to the interplay of both diagrams in Fig. 1, involving genuine flavor violating NU parameters $\alpha_{ij}, i \neq j$.

All in all, the ratio between the expected number of events in the unitary ($\mathcal{N}_{\mathrm{U}}$) and the nonunitary ($\mathcal{N}_{\mathrm{NU}}$) cases is given by

$$\begin{aligned}\frac{\mathcal{N}_{\mathrm{NU}}}{\mathcal{N}_{\mathrm{U}}} &= \mathcal{P}_{\mu e}^{\mathrm{NC}}\frac{G_F^2}{G_\mu^2} + \mathcal{O}(\varepsilon^4) = \frac{(NN^\dagger NN^\dagger NN^\dagger)_{\mu\mu}}{(NN^\dagger)_{ee}(NN^\dagger)_{\mu\mu}} \\ &\approx 2\alpha_{22}^2 - \alpha_{11}^2.\end{aligned} \tag{19}$$

Notice that, contrary to naive expectations, Eq. (19) can be either bigger or smaller than 1, due to the effect of the redefinition of $G_F$. Ideally, though, with very high statistics, one would be sensitive to the $T$-dependence change in the differential cross section at $\mathcal{O}(\varepsilon^4)$ of Eq. (11).

### B. Neutrino-induced muon production

For sufficiently energetic ($E_\nu > 10$ GeV) incoming neutrinos, an additional process with a muon in the final state becomes kinematically possible.

As shown in Fig. 2, there is only one (CC) diagram contributing to this process. Therefore, its kinematical structure is not modified at any order in the seesaw expansion,

$$\sigma^{(\mathrm{SM})} \approx \frac{G_F^2}{\pi}\left(2E_\nu m_e - m_\mu^2\right), \tag{20}$$

so that the effect of nonunitarity translates only into an overall probability factor,

$$\mathcal{P}_{\mu\mu} = (NN^\dagger)_{\mu\mu}^2(NN^\dagger)_{ee} \approx 2\alpha_{22}^2 + \alpha_{11}^2 - 2 \sim 1 - \mathcal{O}(\varepsilon^2). \tag{21}$$

Taking into account also the redefinition of $G_F$ we get

$$\frac{\mathcal{N}_{\mathrm{NU}}}{\mathcal{N}_{\mathrm{U}}} = \mathcal{P}_{\mu\mu}\frac{G_F^2}{G_\mu^2} = (NN^\dagger)_{\mu\mu} \approx \alpha_{22}^2 \leq 1. \tag{22}$$

In summary, leptonic probes such as electron-neutrino elastic scattering and neutrino-induced muon production have a rich phenomenology and a theoretically interesting structure that allows us to probe nonunitarity effects in a unique manner, as shown in Eqs. (11), (19), and (22).

## IV. TESTING NONUNITARITY IN THE NEUTRAL CURRENT AT A NEAR DETECTOR

Long-baseline (LBL) neutrino experiments require a near detector for a reliable flux calibration. They may give the opportunity to measure neutrino-electron scattering with good statistics. For example, DUNE is a planned particle physics experiment aimed at conducting in-depth studies of neutrinos. Scheduled to be hosted by Fermilab in the United States, the project's design includes sending a high-intensity neutrino beam over a distance of approximately 1,300 km from Fermilab in Illinois to a massive liquid-argon time-projection chamber in South Dakota. This far detector will be situated 1.5 km underground at the Sanford Underground Research Facility and is expected to have a total mass of around 40,000 metric tons. DUNE's main goals include investigating neutrino oscillations, exploring $CP$ violation in the leptonic sector, and conducting astrophysical neutrino studies.

Several near detectors are under consideration for DUNE. We will focus our analysis on a detector with similar characteristics as that of the liquid argon near-detector (ND-LAr) located at a distance from the source similar to the one considered at DUNE. In general, near detectors are thought to measure the neutrino beam with high precision. This is essential for reducing systematic uncertainties in the data to be collected by any LBL far detector.

The two detectors will work in tandem, with the near-far configuration enabling more accurate and reliable data interpretation. By providing initial measurements and helping calibrate the far detector's data, DUNE near detectors will be integral to achieving the scientific aims of the DUNE experiment.

The neutrino beam at Fermilab, serving as the neutrino source, can operate in two distinct modes; neutrino and antineutrino. In each mode, the generated beam contains a contribution of four neutrino types; electron neutrinos, electron antineutrinos, muon neutrinos, and muon antineutrinos. Depending on the operation mode, the main contribution is either muon neutrinos or muon antineutrinos in the beam. The main component of the flux, the muon (anti)neutrino, peaks at around 3 GeV, but also contains a long tail extending from 10 GeV to approximately 50 GeV.

In this article, we will delve into a near detector sensitivity to nonunitarity parameters through leptonic processes, taking into account specific design features mentioned above. In order to do so we will analyze the number of events in two distinct processes that can be measured separately; neutrino-electron elastic scattering and neutrino-induced muon production. Notice that the flavor composition of the incoming neutrino is given by the standard flux calculation, while the outgoing neutrinos cannot be distinguished individually and thus we sum over all the kinematically accessible mass states. Moreover, we will restrict ourselves to the leading effects in the seesaw expansion. For example, probing the terms in Eq. (11) that modify the SM kinematical dependence would require measuring the recoil energy of the electrons with a precision way beyond the current envisaged experimental sensitivities for the proposed detectors. As a result, within this approximation, all the effects will depend only on the flavor conserving diagonal couplings $\alpha_{ii}$, and not on the flavour violating ones ($\alpha_{ij}$, $i \neq j$), as argued in Sec. III and Appendix; see for example Eq. (15).

### A. Elastic neutrino-electron scattering

Although the (anti)muon flavor dominates the flux in the (anti)neutrino mode, there are nonzero components of the four flavors/antiflavors involving $e$ and $\mu$. For each process, the number of events in the presence of lepton nonunitarity is calculated as

$$N_a^e = \mathcal{P}_a \mathcal{E} \int_{T_{\min}}^{T_{\max}(E_\nu)} \int_{E_\nu^{\min}(T')}^{\infty} \frac{d\sigma_a}{dT'}(E'_\nu, T')\lambda_a(E_\nu) dE'_\nu dT', \tag{23}$$

where the index $a$ runs over $\{e, \bar{e}, \mu, \bar{\mu}\}$ and $T$ is the detected electron kinetic energy, with the energy threshold in the detector being $T_{\min} = 0.2$ GeV. Here $\lambda_a(E_\nu)$ is the neutrino flux, while $\mathcal{P}_a$ denotes the probability factor of that particular flavor. After neglecting the electron mass compared to $T$ and $E_\nu$ we obtain $E_\nu^{\min}(T) = \frac{1}{2}(T_{\min} + \sqrt{T_{\min}^2 + 2T_{\min} m_e}) \approx T_{\min} = 0.2$ GeV and $T_{\max}(E_\nu) = \frac{2E_\nu^2}{2E_\nu + m_e} \approx E_\nu$. Finally, $\mathcal{E}$ is the exposure, calculated as the product of the number of protons on target per year $1.1 \times 10^{21}$ POT/year, the number of target electrons $N_t = 2 \times 10^{31}$ and the time spent in each mode $t = 3.5$ years. The resulting numbers are given in Table I. We present the expected number of events coming from each neutrino species within the unitary case as well as in the presence of nonunitarity. The probability factor includes the direct effect of the nonunitary lepton mixing matrix as well as the redefinition of $G_F$, expanded to the first order in the seesaw expansion parameter $\varepsilon$.

### B. Neutrino-induced muon production

In order to be kinematically allowed, muon production requires more energetic neutrinos, with the kinematic threshold given by $E_\nu > (m_\mu^2 - m_e^2)/2m_e \approx 10$ GeV. While the flux peaks at a lower energy ~3 GeV, the tails can still generate a significant number of muon events in the final state, thus improving the sensitivity to the nonunitarity parameters. The number of events is given by

$$N_a^\mu = \mathcal{P}_a \mathcal{E} \int_{E_\nu^{\min}}^{\infty} \sigma(E_\nu)\lambda_a(E_\nu) dE_\nu, \tag{24}$$

where, again, $\mathcal{E}$ is the exposure and $\lambda_a(E_\nu)$ is the flux.

Note that now $a$ denotes either the incoming muon neutrino or electron antineutrino. Muon antineutrino and electron neutrino flavors do not contribute to this process in the standard unitary case while, in the presence of nonunitarity, their contribution appears only as order $\mathcal{O}(\varepsilon^4)$ corrections. The results are given in Table II.

### C. Analysis

We now proceed to estimate the sensitivity of our proposed leptonic-probe experiment to the nonunitarity parameters. In order to do so we take the $\chi^2$ function as

$$\chi^2 = \sum_i \frac{(N_i^{\text{the}} - N_i^{\exp})^2}{\sigma_{i,\text{stat}}^2 + \sigma_{i,\text{syst}}^2}, \tag{25}$$

where the subscript $i$ runs over the four possible measurements; electron or muon events during the neutrino or antineutrino modes. Here $N_i^{\exp}$ is the number of detected events, while $N_i^{\text{the}}$ is the expected number of events given as a function of the nonunitarity parameters and $\sigma_{i,\text{stat}}^2 = N_i^{\exp}$.

TABLE I. Expected number of electron events in the unitary case coming from each relevant neutrino type. The detector is sensitive only to the total number of events, but the probability factor in the presence of nonunitarity is different for each incoming (anti)flavor. The error $\sigma$ is taken as $\sigma^2 = \sigma_{\text{stat}}^2 + \sigma_{\text{syst}}^2$, where the statistical uncertainty $\sigma_{\text{stat}} = \sqrt{N}$ and the systematic uncertainty is taken as 2% (see text for details).

| $\mathcal{N}_{\text{U}}$ | $\nu$ mode | | $\bar{\nu}$ mode | | $\mathcal{N}_{\text{NU}}/\mathcal{N}_{\text{U}}$ | | |
|---|---|---|---|---|---|---|---|
| $\nu_a + e^- \to \nu_j + e^-$ | Events | $\sigma$ | Events | $\sigma$ | $\mathcal{P}G_F^2/G_\mu^2$ | Seesaw order | Main contribution |
| $\nu_e$ | 2,800 | 80 | 1,530 | 50 | $2\alpha_{11}^2 - \alpha_{22}^2$ | $1 \pm \mathcal{O}(\varepsilon^2)$ | NC + CC |
| $\nu_\mu$ | 31,400 | 700 | 5,800 | 100 | $2\alpha_{22}^2 - \alpha_{11}^2$ | $1 \pm \mathcal{O}(\varepsilon^2)$ | NC |
| $\bar{\nu}_e$ | 430 | 20 | 780 | 30 | $2\alpha_{11}^2 - \alpha_{22}^2$ | $1 \pm \mathcal{O}(\varepsilon^2)$ | NC + CC |
| $\bar{\nu}_\mu$ | 3,200 | 80 | 20,000 | 400 | $2\alpha_{22}^2 - \alpha_{11}^2$ | $1 \pm \mathcal{O}(\varepsilon^2)$ | NC |
| *Total* | 37,800 | 800 | 28,000 | 600 | | | |

TABLE II. Expected number of muon events in the unitary case coming from each species. The detector is sensitive only to the total event number, but the probability factor in the presence of nonunitarity differs for each incoming (anti)flavor. $\sigma$ is $\sigma^2 = \sigma_{\rm stat}^2 + \sigma_{\rm syst}^2$, where $\sigma_{\rm stat} = \sqrt{N}$ and the systematic uncertainty is taken as 2% (see text for details).

| $\mathcal{N}_{\rm U}$ | $\nu$ mode | | $\bar{\nu}$ mode | | $\mathcal{N}_{\rm NU}/\mathcal{N}_{\rm U}$ | | |
|---|---|---|---|---|---|---|---|
| $\nu_a + e^- \to \nu_j + \mu^-$ | Events | $\sigma$ | Events | $\sigma$ | $\mathcal{P}G_F^2/G_\mu^2$ | Seesaw order | Main contribution |
| $\nu_e$ | 0 | 0 | 0 | 0 | $\lvert\alpha_{21}\rvert^2$ | $\mathcal{O}(\varepsilon^4)$ | $\mathcal{O}(\varepsilon^4)$ |
| $\nu_\mu$ | 17,900 | 400 | 14,200 | 300 | $\alpha_{22}^2$ | $1 - \mathcal{O}(\varepsilon^2)$ | CC |
| $\bar{\nu}_e$ | 380 | 20 | 230 | 20 | $\alpha_{11}^2$ | $1 - \mathcal{O}(\varepsilon^2)$ | CC |
| $\bar{\nu}_\mu$ | 0 | 0 | 0 | 0 | $\lvert\alpha_{21}\rvert^2$ | $\mathcal{O}(\varepsilon^4)$ | $\mathcal{O}(\varepsilon^4)$ |
| *Total* | 18,300 | 400 | 14,400 | 300 | | | |

In the analysis we will take different possible values for the systematic error, ranging from 0–3%, in order to account for the uncertainty in the flux calculation. We are aware that our benchmark assumption is too optimistic for the current setup, but it should serve as motivation for improvement, given the interest of the associated physics.

Notice that nonunitarity accounts for the fact that the heavy mediator states are not kinematically accessible. The direct effects of nonunitarity tend to decrease the event number, and this goes in the opposite direction as the redefinition of the Fermi constant $G_F$ discussed above. As a result, there is an intrinsic ambiguity in the electron events alone, leading to a parameter degeneracy. Note however that this ambiguity is not present in the charged current events, which are only sensitive to $\alpha_{22}^2$. Hence one can obtain a limit for both $\alpha_{11}^2$ and $\alpha_{22}^2$ only combining CC and NC event types. This behavior can be seen in Fig. 3 where, for illustration purposes, an optimistic $\sigma = \sigma_{\rm stat}$ uncertainty was assumed. We compare the recently updated "neutrino limits" extracted from neutrino oscillations at both long and short baseline experiments [47–50].

A few additional comments are in order. A realistic sensitivity estimate would require a detailed study of the background. In several background analysis discussions of neutrino-electron scattering experiments, a common cut is to select events with small values for the $E\theta^2$ variable (see for instance [51]).

On the other hand, hadronic processes will also be sensitive to nonunitarity effects [43] and will dominate the statistics compared with neutrino electron scattering (for a recent discussion see [52]). The results of both analyses will be complementary, as the dependence on the nonunitarity parameters will be different. In particular, the effects discussed here are $K^6$ and involve an interference

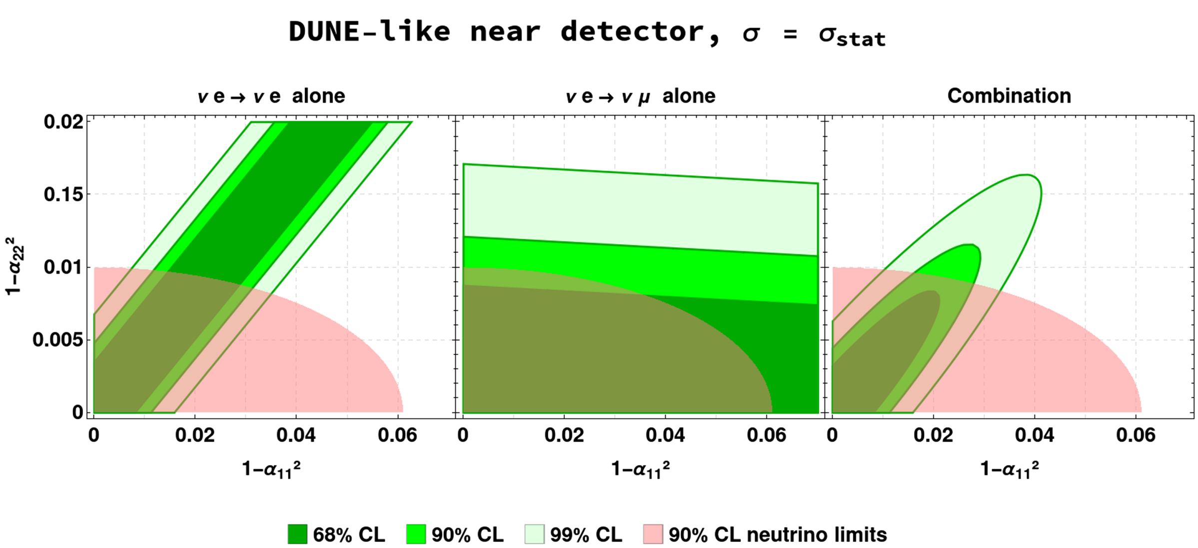


FIG. 3. Sensitivities on the parameters $\alpha_{11}$ and $\alpha_{22}$ from our suggested DUNE-like near detector. The neutral current-dominated elastic neutrino-electron scattering process constrains the quantity $2\alpha_{22}^2 - \alpha_{11}^2$ (left panel), while the purely charged current process $\nu_\mu + e^- \to \nu_j + \mu^-$ involves only $\alpha_{22}^2$ (middle panel). The combination of both event types in the lepton channel constrains both nonunitarity parameters $\alpha_{11}^2$ and $\alpha_{22}^2$ (right panel). As a benchmark, we show the sensitivity of a hypothetical experiment where the statistical uncertainty dominates over the systematics. For comparison, the pink region represents the constraints from both long and short baseline experiments, as detailed in [47].

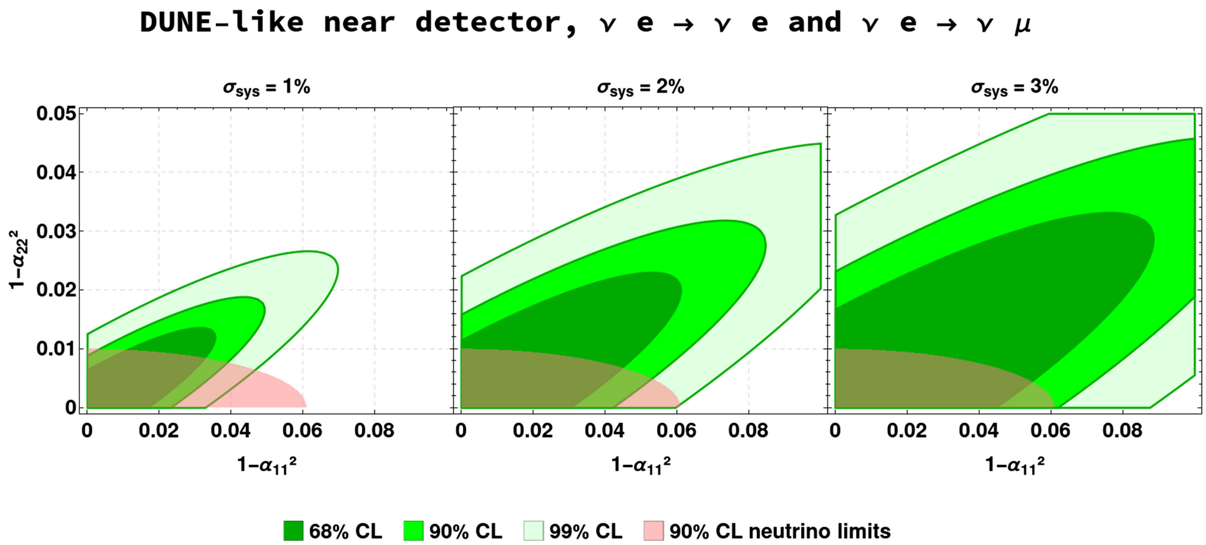


FIG. 4. Combination of the NC ($\nu + e \to \nu + e$) and CC ($\nu + e \to \nu + \mu$) results for different values of the systematic uncertainty. Again, the pink region represents the constraints from both long and short baseline experiments [47]. While the constraints on $\alpha_{22}^2$ are already strong, this setup has the potential to significantly improve also the one on $\alpha_{11}^2$.

between the CC and NC, while the hadronic processes are either purely NC and $K^6$, or purely CC and $K^4$. Note that, despite having smaller statistics, neutrino-electron scattering will be a cleaner process as it is purely weak, free of strong corrections, so its cross section uncertainties will be smaller than for the hadronic case.

In any case, our goal here is to focus more on the novelty of the measurement, rather that on the strength of the resulting sensitivities, as the setup is currently not optimized to do so. However, we can see that the attainable results can already be comparable to other similar experiments. In particular, the $\alpha_{11}^2$ can be probed significantly better than current oscillation experiments [47]. It is worth noting that in general there are constraints arising from universality tests [53], electroweak precision measurements [54], such as the invisible Z decay [55], and charged-lepton flavor-violation searches [56,57]. For a recent extensive discussion see [58]. While the combination of these restrictions can be rather stringent, we stress the cleanliness of our proposed leptonic probe, and the fact that the interpretation is fairly model-independent.

In Fig. 4 we now consider the role of different values of the systematic uncertainty and again compare the resulting sensitivities with the current oscillation constraint.

Finally, we note that by combining the results from a DUNE-like near detector with the oscillation constraints for different values of the systematic uncertainty, the measurement for $\alpha_{11}^2$ can indeed improve, see Fig. 5. The fact that this happens even when the setup is not optimized for this type of measurement should serve as a motivation for the design of future experiments using leptonic neutral current as a way to underpin the neutrino mass generation seesaw mechanism.

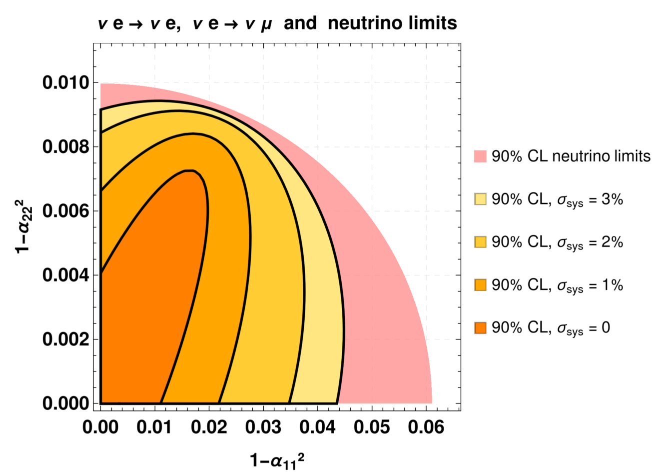


FIG. 5. Combination of our proposed DUNE-like near detector measurements, i.e., neutrino electron scattering and neutrino induced muon production, with the long and short baseline oscillation experiments constraints of [47] at 90% CL for different values of the systematic uncertainty.

## V. CONCLUSIONS AND OUTLOOK

Here we have proposed the use of leptonic probes, such as neutrino-electron scattering, as a viable way to test the nonminimal form of the charged and neutral leptonic weak interactions within a DUNE-like near-detector setup. Although the statistics is low, these processes are very clean and can provide complementary information to that available from oscillation studies. While the current setup is not optimized to our proposal, our results already indicate that there is potential for significant improvement on the sensitivities for the nonunitarity parameter $\alpha_{11}^2$ when compared with current oscillation experiments. For example, Figs. 3–5 illustrate how our method can help improving nonunitarity constraints and thereby shed light on the scale of neutrino mass generation within low-scale seesaw schemes. Last, but not least, our results further highlight the fact that a robust experimental setup for neutrino research requires the presence of near detectors. In addition to ensuring robustness, these short-distance studies can provide, by themselves, valuable information on new physics parameters, such as the nonunitarity parameters, which constitutes an interesting physics goal by itself. Besides a plethora of low-energy probes [36–42], there are plenty of physics opportunities for testing unitarity violation. For example, through the searches for charged-lepton flavor-violating processes at low and high energies [59–62]. One may also have the possibility of directly producing the TeV scale neutrino-mass-mediators at colliders [63–74]. The rich variety of associated signals justifies the intense experimental effort devoted in present and upcoming experiments [75–81].

## ACKNOWLEDGMENTS

We thank Joachim Kopp and Jaehoon Yu for insightful discussions. This work was supported by the Spanish Grants No. PID2020–113775GB-I00 (AEI) and No. Prometeo CIPROM/2021/054 (Generalitat Valenciana). O. G. M. was supported by the Consejo Nacional de Humanidades, Ciencias y Tecnologías (CONAHCyT) Grant No. 23238 and by Sistema Nacional de Investigadoras e Investigadores (SNII)-México.

## APPENDIX: GENERAL FORMALISM FOR NEUTRINO AND ANTINEUTRINO SCATTERING

Here we consider the general family of neutrino scattering processes $\nu_\alpha + e^- \to \nu + \ell_\beta^-$ and $\bar{\nu}_\alpha + e^- \to \bar{\nu} + \ell_\beta^-$ where $\alpha$ denotes the initial (anti)neutrino flavor, and the final lepton $\ell_\beta^-$ can be an electron, a muon or a tau, if kinematically possible. In other words, the initial (anti)neutrino is produced in association with a charged lepton of definite flavor. Moreover the neutrinos mix with new heavy mediator states. Since the final (anti)neutrino state is not measured,we sum over the three kinematically accessible neutral mass states $j$. We discuss the effect of nonunitarity at zero distance.

At tree level there is always a nonzero contribution coming from the charged current irrespective of $\alpha$ and $\beta$. However, we show that the cases in which this contribution vanishes in the unitary case are actually of order $\mathcal{O}(\varepsilon^4)$ in the presence of nonunitarity. On the other hand, when the probability factor is 1 in the standard case one now has a modification by a common factor of order $1 - \mathcal{O}(\varepsilon^2)$. For the NC there is only a nonzero contribution if $\beta = e$, in which case it is always of order $1 - \mathcal{O}(\varepsilon^2)$.

### 1. Neutrino scattering

The full structure of the relevant diagrams is shown in the upper row of Fig. 6, while the relevant probability (and interference) factors are given in Eqs. (A1)–(A3). Note that the probability factors are different for each combination of diagrams, i.e.,

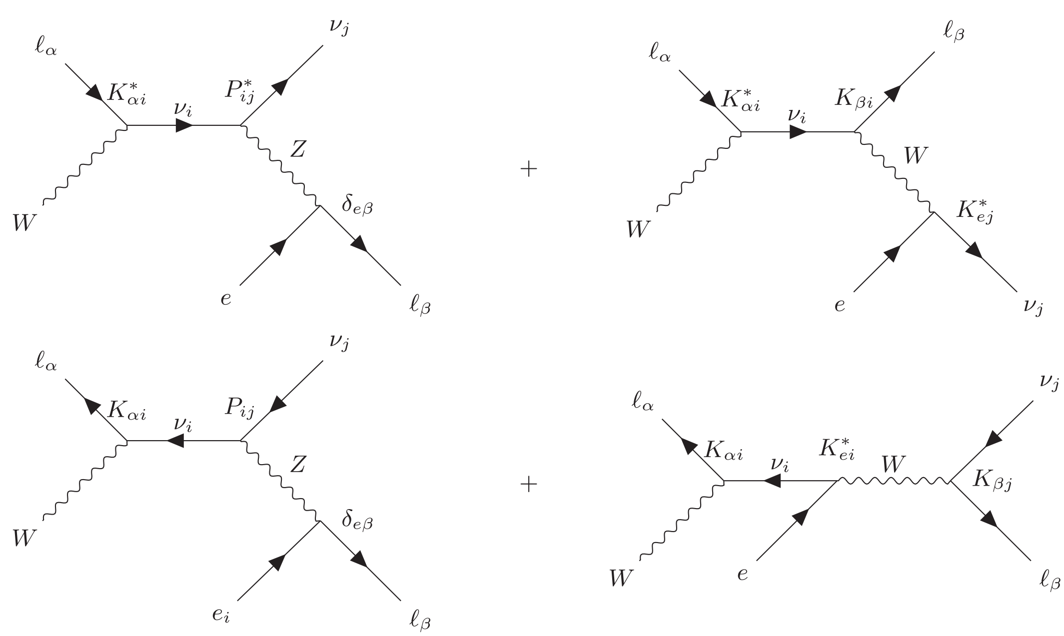


FIG. 6. Interplay between charged and neutral currents in the processes $\nu_\alpha + e^- \to \nu + \ell_\beta^-$ (upper row) and $\bar{\nu}_\alpha + e^- \to \bar{\nu} + \ell_\beta^-$ (lower row). The standard probability factors for each diagram are either 1 or 0, depending on the initial flavor $\alpha$ and the final charged lepton $\ell_\beta$. However, in the presence of nonunitarity both diagrams are present, each carrying a different probability factor. Within a consistent seesaw expansion we show that the SM kinematic structure is preserved at order $\mathcal{O}(\varepsilon^2)$ (see text for details).

$$\mathcal{P}^{\mathrm{NC}}_{\alpha\beta} = \delta_{e\beta}(NN^\dagger NN^\dagger NN^\dagger)_{\alpha\alpha}, \tag{A1}$$

$$\mathcal{P}^{\mathrm{CC}}_{\alpha\beta} = (NN^\dagger)_{\alpha\beta}(NN^\dagger)_{\beta\alpha}(NN^\dagger)_{ee}, \tag{A2}$$

$$\mathcal{P}^{\mathrm{int}}_{\alpha\beta} = \delta_{e\beta}(NN^\dagger)_{\beta\alpha}(NN^\dagger NN^\dagger)_{\alpha e}. \tag{A3}$$

Notice that $\alpha$ and $\beta$ denote the fixed flavor indices associated to the survival or conversion probability, while the latin indices $i$, $j$ are summed over, that is

$$(NN^\dagger)_{\alpha\beta} = \sum_{j=1}^{3} N_{\alpha j}N^\dagger_{j\beta}.$$

Each of the probability factors in Eqs. (A1)–(A3) affects different terms in the cross section, making the complete expression a complicated one. However, as already discussed for the particular $\nu_\mu$-electron elastic scattering case in Sec. III A, one finds that in general the kinematic structure of the SM is preserved at order $\mathcal{O}(\varepsilon^2)$. Modifications to the SM spectrum shape only come at order $\mathcal{O}(\varepsilon^4)$. For example, up to $\mathcal{O}(\varepsilon^2)$, one finds

$$\mathcal{P}^{\mathrm{NC}}_{\alpha\beta} \approx \delta_{e\beta}(3\alpha^2_{\alpha\alpha} - 2) + \mathcal{O}(\varepsilon^4) \sim \delta_{e\beta} \times [1 - \mathcal{O}(\varepsilon^2)], \tag{A4}$$

$$\mathcal{P}^{\mathrm{CC}}_{\alpha\beta} \approx \delta_{\alpha\beta}(2\alpha^2_{\alpha\alpha} + \alpha^2_{11} - 2) + \mathcal{O}(\varepsilon^4) \sim \delta_{\alpha\beta} \times [1 - \mathcal{O}(\varepsilon^2)], \tag{A5}$$

$$\mathcal{P}^{\mathrm{int}}_{\alpha\beta} \approx \delta_{e\beta}\delta_{\alpha\beta}(3\alpha^2_{11} - 2) + \mathcal{O}(\varepsilon^4) \sim \delta_{e\beta}\delta_{\alpha\beta} \times [1 - \mathcal{O}(\varepsilon^2)]. \tag{A6}$$

From these one can easily conclude:

(i) In inelastic scattering processes (muon or tau neutrino-induced production), where the final charged lepton is not an electron, only the CC contribution exists. This corresponds to the case $\beta \neq e$.

(ii) In elastic neutrino-electron scattering, $\beta = e$, if the initial neutrino flavor is of $\mu$ or $\tau$ type, $\alpha \neq e$, there is a CC contribution of order $\mathcal{O}(\varepsilon^4)$, subleading in comparison to the neutral current.

(iii) If $\beta = e$ and the initial neutrino flavor is of electron type, $\alpha = e$, then the probability factors of the NC, the CC and the interference are all equal to $3\alpha^2_{11} - 2$. This means that, again, there is no spectral distortion at order $\mathcal{O}(\varepsilon^2)$.

We emphasize that at tree level and $\mathcal{O}(\varepsilon^2)$ in the seesaw expansion parameter the effect of nonunitarity is just a global factor times the SM prediction. This conclusion no longer holds at second order in the seesaw expansion, when the flavor-violating parameters of Eq. (3) come into play. In this case the $\mathcal{N}_{\mathrm{NU}}/\mathcal{N}_{\mathrm{U}}$ event number ratio will not be a constant and will instead depend on the kinematic parameters and flux shape.

A summary of these results is given in Table III, and the SM cross sections are given by

$$\frac{d\sigma^{\mathrm{NC+CC}}}{dT}(\nu + e^- \to \nu + e^-) = \frac{2G_F^2 m_e}{\pi}\left((1+g_L)^2 + g_R^2\left(1 - \frac{T}{E\nu}\right)^2 - (1+g_L)g_R\frac{m_e T}{E_\nu^2}\right), \tag{A7}$$

$$\frac{d\sigma^{\mathrm{NC}}}{dT}(\nu + e^- \to \nu + e^-) = \frac{2G_F^2 m_e}{\pi}\left(g_L^2 + g_R^2\left(1 - \frac{T}{E\nu}\right)^2 - g_L g_R\frac{m_e T}{E_\nu^2}\right), \tag{A8}$$

$$\sigma(\nu + e^- \to \nu + \mu^-) = \frac{G_F^2}{\pi}(2E_\nu m_e - m_\mu^2), \tag{A9}$$

$$\sigma(\nu + e^- \to \nu + \tau^-) = \frac{G_F^2}{\pi}(2E_\nu m_e - m_\tau^2). \tag{A10}$$

TABLE III. Structure of the family of processes $\nu_\alpha + e^- \to \nu + \ell^-_\beta$ in the presence of nonunitarity, including the probability factors at order $\mathcal{O}(\varepsilon^2)$, the kinematic factors for each contribution: NC, CC, or the interference.

| Process | Contribution | $\mathcal{P}$ factor at $\mathcal{O}(\varepsilon^2)$ | $\mathcal{N}_{\mathrm{NU}}/\mathcal{N}_{\mathrm{U}} = \mathcal{P}G_F^2/G_\mu^2$ | SM cross section | Kinematic threshold (Lab) |
|---|---|---|---|---|---|
| $\nu_e + e^- \to \nu_j + e^-$ | NC + CC | $3\alpha^2_{11} - 2$ | $2\alpha^2_{11} - \alpha^2_{22}$ | Eq. (A7) | |
| $\nu_\mu + e^- \to \nu_j + e^-$ | NC | $3\alpha^2_{22} - 2$ | $2\alpha^2_{22} - \alpha^2_{11}$ | Eq. (A8) | No |
| $\nu_\tau + e^- \to \nu_j + e^-$ | NC | $3\alpha^2_{33} - 2$ | $3\alpha^2_{33} - \alpha^2_{22} - \alpha^2_{11}$ | Eq. (A8) | |
| $\nu_e + e^- \to \nu_j + \mu^-$ | | $\mathcal{O}(\varepsilon^4)$ | $\mathcal{O}(\varepsilon^4)$ | | |
| $\nu_\mu + e^- \to \nu_j + \mu^-$ | CC | $2\alpha^2_{22} + \alpha^2_{11} - 2$ | $\alpha^2_{22}$ | Eq. (A9) | $E_\nu > 10$ GeV |
| $\nu_\tau + e^- \to \nu_j + \mu^-$ | | $\mathcal{O}(\varepsilon^4)$ | $\mathcal{O}(\varepsilon^4)$ | | |
| $\nu_e + e^- \to \nu_j + \tau^-$ | | $\mathcal{O}(\varepsilon^4)$ | $\mathcal{O}(\varepsilon^4)$ | | |
| $\nu_\mu + e^- \to \nu_j + \tau^-$ | | $\mathcal{O}(\varepsilon^4)$ | $\mathcal{O}(\varepsilon^4)$ | | $E_\nu > 3$ TeV |
| $\nu_\tau + e^- \to \nu_j + \tau^-$ | CC | $2\alpha^2_{33} + \alpha^2_{11} - 2$ | $2\alpha^2_{33} - \alpha^2_{22}$ | Eq. (A10) | |

TABLE IV. Summary of the family of processes $\bar{\nu}_\alpha + e^- \to \bar{\nu} + \ell_\beta^-$ in the presence of nonunitarity, including the probability factors at order $\mathcal{O}(\varepsilon^2)$, the kinematic factors and the contribution type; NC, CC, or the interference.

| Process | Contribution | $\mathcal{P}$ factor at $\mathcal{O}(\varepsilon^2)$ | $\mathcal{N}_{\rm NU}/\mathcal{N}_{\rm U} = \mathcal{P}G_F^2/G_\mu^2$ | SM cross section | Kinematic threshold (Lab) |
|---|---|---|---|---|---|
| $\bar{\nu}_e + e^- \to \bar{\nu}_j + e^-$ | NC + CC | $3\alpha_{11}^2 - 2$ | $2\alpha_{11}^2 - \alpha_{22}^2$ | Eq. (A7), $(1+g_L) \leftrightarrow g_R$ | |
| $\bar{\nu}_\mu + e^- \to \bar{\nu}_j + e^-$ | NC | $3\alpha_{22}^2 - 2$ | $2\alpha_{22}^2 - \alpha_{11}^2$ | Eq. (A8), $g_L \leftrightarrow g_R$ | No |
| $\bar{\nu}_\tau + e^- \to \bar{\nu}_j + e^-$ | NC | $3\alpha_{33}^2 - 2$ | $3\alpha_{33}^2 - \alpha_{22}^2 - \alpha_{11}^2$ | Eq. (A8), $g_L \leftrightarrow g_R$ | |
| $\bar{\nu}_e + e^- \to \bar{\nu}_j + \mu^-$ | CC | $2\alpha_{11}^2 + \alpha_{22}^2 - 2$ | $\alpha_{11}^2$ | Eq. (A9) | |
| $\bar{\nu}_\mu + e^- \to \bar{\nu}_j + \mu^-$ | | $\mathcal{O}(\varepsilon^4)$ | $\mathcal{O}(\varepsilon^4)$ | | $E_\nu > 10$ GeV |
| $\bar{\nu}_\tau + e^- \to \bar{\nu}_j + \mu^-$ | | $\mathcal{O}(\varepsilon^4)$ | $\mathcal{O}(\varepsilon^4)$ | | |
| $\bar{\nu}_e + e^- \to \bar{\nu}_j + \tau^-$ | CC | $2\alpha_{11}^2 + \alpha_{33}^2 - 2$ | $\alpha_{11}^2 - \alpha_{22}^2 + \alpha_{33}^2$ | Eq. (A10) | |
| $\bar{\nu}_\mu + e^- \to \bar{\nu}_j + \tau^-$ | | $\mathcal{O}(\varepsilon^4)$ | $\mathcal{O}(\varepsilon^4)$ | | $E_\nu > 3$ TeV |
| $\bar{\nu}_\tau + e^- \to \bar{\nu}_j + \tau^-$ | | $\mathcal{O}(\varepsilon^4)$ | $\mathcal{O}(\varepsilon^4)$ | | |

### 2. Antineutrino scattering

While the results will be very similar to the neutrino case, we include them here for completeness. The diagrams are slightly different and are given by the lower row of Fig. 6, while their respective probability factors (and the interference) are given in Eqs. (A11)–(A13).

$$\mathcal{P}_{\alpha\beta}^{\rm NC} = \delta_{e\beta}(NN^\dagger NN^\dagger NN^\dagger)_{\alpha\alpha}, \tag{A11}$$

$$\mathcal{P}_{\alpha\beta}^{\rm CC} = (NN^\dagger)_{\alpha e}(NN^\dagger)_{e\alpha}(NN^\dagger)_{\beta\beta}, \tag{A12}$$

$$\mathcal{P}_{\alpha\beta}^{\rm int} = \delta_{e\beta}(NN^\dagger)_{e\alpha}(NN^\dagger NN^\dagger)_{\alpha\beta}, \tag{A13}$$

i.e., just replacing $e \leftrightarrow \beta$ in the neutrino case. Similar conclusions apply and a summary can be found in Table IV.


[1] T. Kajita, Nobel lecture: Discovery of atmospheric neutrino oscillations, Rev. Mod. Phys. **88**, 030501 (2016).
[2] A. B. McDonald, Nobel lecture: The Sudbury Neutrino Observatory: Observation of flavor change for solar neutrinos, Rev. Mod. Phys. **88**, 030502 (2016).
[3] D. Akimov *et al.* (COHERENT Collaboration), Observation of coherent elastic neutrino-nucleus scattering, Science **357**, 1123 (2017).
[4] D. Akimov *et al.* (COHERENT Collaboration), COHERENT Collaboration data release from the first observation of coherent elastic neutrino-nucleus scattering, arXiv:1804.09459.
[5] D. Z. Freedman, Coherent neutrino nucleus scattering as a probe of the weak neutral current, Phys. Rev. D **9**, 1389 (1974).
[6] A. Drukier and L. Stodolsky, Principles and applications of a neutral current detector for neutrino physics and astronomy, Phys. Rev. D **30**, 2295 (1984).
[7] J. Schechter and J. W. F. Valle, Neutrino masses in $\mathrm{SU}(2) \times \mathrm{U}(1)$ theories, Phys. Rev. D **22**, 2227 (1980).
[8] J. Schechter and J. W. F. Valle, Neutrino decay and spontaneous violation of lepton number, Phys. Rev. D **25**, 774 (1982).
[9] J. W. F. Valle, Resonant oscillations of massless neutrinos in matter, Phys. Lett. B **199**, 432 (1987).
[10] H. Nunokawa, Y.-Z. Qian, A. Rossi, and J. W. F. Valle, Resonant conversion of massless neutrinos in supernovae, Phys. Rev. D **54**, 4356 (1996).
[11] D. Grasso, H. Nunokawa, and J. W. F. Valle, Pulsar velocities without neutrino mass, Phys. Rev. Lett. **81**, 2412 (1998).
[12] R. Mohapatra and J. W. F. Valle, Neutrino mass and baryon number nonconservation in superstring models, Phys. Rev. D **34**, 1642 (1986).
[13] M. Gonzalez-Garcia and J. W. F. Valle, Fast decaying neutrinos and observable flavor violation in a new class of Majoron models, Phys. Lett. B **216**, 360 (1989).
[14] E. K. Akhmedov, M. Lindner, E. Schnapka, and J. W. F. Valle, Left-right symmetry breaking in NJL approach, Phys. Lett. B **368**, 270 (1996).
[15] E. K. Akhmedov *et al.*, Dynamical left-right symmetry breaking, Phys. Rev. D **53**, 2752 (1996).
[16] M. Malinsky, J. Romao, and J. W. F. Valle, Novel supersymmetric SO(10) seesaw mechanism, Phys. Rev. Lett. **95**, 161801 (2005).
[17] F. Escrihuela, D. V. Forero, O. G. Miranda, M. Tórtola, and J. W. F. Valle, On the description of nonunitary neutrino mixing, Phys. Rev. D **92**, 053009 (2015).
[18] F. Escrihuela, D. Forero, O. Miranda, M. Tórtola, and J. W. F. Valle, Probing CP violation with non-unitary mixing

in long-baseline neutrino oscillation experiments: DUNE as a case study, New J. Phys. **19**, 093005 (2017).
[19] C. S. Fong, H. Minakata, and H. Nunokawa, A framework for testing leptonic unitarity by neutrino oscillation experiments, J. High Energy Phys. 02 (2017) 114.
[20] S.-F. Ge, P. Pasquini, M. Tortola, and J. W. F. Valle, Measuring the leptonic *CP* phase in neutrino oscillations with nonunitary mixing, Phys. Rev. D **95**, 033005 (2017).
[21] O. Miranda and J. W. F. Valle, Neutrino oscillations and the seesaw origin of neutrino mass, Nucl. Phys. **B908**, 436 (2016).
[22] O. Miranda, M. Tortola, and J. W. F. Valle, New ambiguity in probing *CP* violation in neutrino oscillations, Phys. Rev. Lett. **117**, 061804 (2016).
[23] C. S. Fong, H. Minakata, and H. Nunokawa, Non-unitary evolution of neutrinos in matter and the leptonic unitarity test, J. High Energy Phys. 02 (2019) 015.
[24] L. S. Miranda, P. Pasquini, U. Rahaman, and S. Razzaque, Searching for non-unitary neutrino oscillations in the present T2K and NO$\nu$A data, Eur. Phys. J. C **81**, 444 (2021).
[25] O. G. Miranda, D. K. Papoulias, O. Sanders, M. Tórtola, and J. W. F. Valle, Future CEvNS experiments as probes of lepton unitarity and light-sterile neutrinos, Phys. Rev. D **102**, 113014 (2020).
[26] I. Martinez-Soler and H. Minakata, Measuring tau neutrino appearance probability via unitarity, Phys. Rev. D **104**, 093006 (2021).
[27] U. Rahaman and S. Razzaque, Non-unitary neutrino mixing in the NO$\nu$A near detector data, Universe **8**, 238 (2022).
[28] C. Soumya, Probing nonunitary neutrino mixing via long-baseline neutrino oscillation experiments based at J-PARC, Phys. Rev. D **105**, 015012 (2022).
[29] D. Kaur, N. R. K. Chowdhury, and U. Rahaman, Effect of non-unitary mixing on the mass hierarchy and CP violation determination at the Protvino to Orca experiment, Eur. Phys. J. C **84**, 118 (2024).
[30] Y. Wang and S. Zhou, Non-unitary leptonic flavor mixing and CP violation in neutrino-antineutrino oscillations, Phys. Lett. B **824**, 136797 (2022).
[31] S. S. Chatterjee, O. G. Miranda, M. Tórtola, and J. W. F. Valle, Nonunitarity of the lepton mixing matrix at the European Spallation Source, Phys. Rev. D **106**, 075016 (2022).
[32] S. Gariazzo, P. Martínez-Miravé, O. Mena, S. Pastor, and M. Tórtola, Non-unitary three-neutrino mixing in the early Universe, J. Cosmol. Astropart. Phys. 03 (2023) 046.
[33] D. Aloni and A. Dery, Revisiting leptonic non-unitarity, Phys. Rev. D **109**, 055006 (2024).
[34] S. Sahoo, S. Das, A. Kumar, and S. K. Agarwalla, Constraining non-unitary neutrino mixing using matter effects in atmospheric neutrinos at INO-ICAL, arXiv:2309.16942.
[35] J. M. Celestino-Ramírez, F. J. Escrihuela, L. J. Flores, and O. G. Miranda, Testing the non-unitarity of the leptonic mixing matrix at FASER$\nu$ and FASER$\nu$2, Phys. Rev. D **109**, L011705 (2024).
[36] O. G. Miranda, D. K. Papoulias, O. Sanders, M. Tórtola, and J. W. F. Valle, Low-energy probes of sterile neutrino transition magnetic moments, J. High Energy Phys. 12 (2021) 191.
[37] T. Schwetz and A. Segarra, T violation in nonstandard neutrino oscillation scenarios, Phys. Rev. D **105**, 055001 (2022).
[38] T. Schwetz and A. Segarra, Model-independent test of T violation in neutrino oscillations, Phys. Rev. Lett. **128**, 091801 (2022).
[39] J. Tang, S. Vihonen, and Y. Xu, Precision measurements and $\tau$ neutrino physics in a future accelerator neutrino experiment, Commun. Theor. Phys. **74**, 035201 (2022).
[40] J. Arrington *et al.*, Physics opportunities for the Fermilab booster replacement, arXiv:2203.03925.
[41] F. Capozzi, C. Giunti, and C. A. Ternes, Improved sensitivities of ESS$\nu$SB from a two-detector fit, J. High Energy Phys. 04 (2023) 130.
[42] S. R. Soleti, P. Coloma, J. J. G. Cadenas, and A. Cabrera, Search for hidden neutrinos at the European Spallation Source: The SHiNESS experiment, J. High Energy Phys. 03 (2024) 148.
[43] O. Miranda, P. Pasquini, M. Tórtola, and J. W. F. Valle, Exploring the potential of short-baseline physics at Fermilab, Phys. Rev. D **97**, 095026 (2018).
[44] P. Coloma, J. López-Pavón, S. Rosauro-Alcaraz, and S. Urrea, New physics from oscillations at the DUNE near detector, and the role of systematic uncertainties, J. High Energy Phys. 08 (2021) 065.
[45] P. de Salas, D. V. Forero, S. Gariazzo, P. Martínez-Miravé, O. Mena, C. A. Ternes, M. Tórtola, and J. W. F. Valle, 2020 global reassessment of the neutrino oscillation picture, J. High Energy Phys. 02 (2021) 071.
[46] M. Blennow, P. Coloma, E. Fernandez-Martinez, J. Hernandez-Garcia, and J. Lopez-Pavon, Non-unitarity, sterile neutrinos, and non-standard neutrino interactions, J. High Energy Phys. 04 (2017) 153.
[47] D. Forero, C. Giunti, C. Ternes, and M. Tortola, Non-unitary neutrino mixing in short and long-baseline experiments, Phys. Rev. D **104**, 075030 (2021).
[48] Z. Hu, J. Ling, J. Tang, and T. Wang, Global oscillation data analysis on the 3$\nu$ mixing without unitarity, J. High Energy Phys. 01 (2021) 124.
[49] S. A. R. Ellis, K. J. Kelly, and S. W. Li, Current and future neutrino oscillation constraints on leptonic unitarity, J. High Energy Phys. 12 (2020) 068.
[50] S. K. Agarwalla, S. Das, A. Giarnetti, and D. Meloni, Model-independent constraints on non-unitary neutrino mixing from high-precision long-baseline experiments, J. High Energy Phys. 07 (2022) 121.
[51] L. Zazueta *et al.* (MINERvA Collaboration), Improved constraint on the MINER$\nu$A medium energy neutrino flux using $\bar{\nu}e^- \to \bar{\nu}e^-$ data, Phys. Rev. D **107**, 012001 (2023).
[52] V. Hewes *et al.* (DUNE Collaboration), Deep Underground Neutrino Experiment (DUNE) near detector conceptual design report, Instrum. Exp. Tech. **5**, 31 (2021).
[53] D. Bryman, V. Cirigliano, A. Crivellin, and G. Inguglia, Testing lepton flavor universality with pion, kaon, tau, and beta decays, Annu. Rev. Nucl. Part. Sci. **72**, 69 (2022).
[54] R. L. Workman *et al.* (Particle Data Group), Review of particle physics, Prog. Theor. Exp. Phys. **2022**, 083C01 (2022).
[55] F. J. Escrihuela, L. J. Flores, and O. G. Miranda, Neutrino counting experiments and non-unitarity from LEP and future experiments, Phys. Lett. B **802**, 135241 (2020).

[56] D. Forero, S. Morisi, M. Tortola, and J. W. F. Valle, Lepton flavor violation and non-unitary lepton mixing in low-scale type-I seesaw, J. High Energy Phys. 09 (2011) 142.

[57] M. Lindner, M. Platscher, and F. S. Queiroz, A call for new physics: The muon anomalous magnetic moment and lepton flavor violation, Phys. Rep. **731**, 1 (2018).

[58] M. Blennow, E. Fernández-Martínez, J. Hernández-García, J. López-Pavón, X. Marcano, and D. Naredo-Tuero, Bounds on lepton non-unitarity and heavy neutrino mixing, J. High Energy Phys. 08 (2023) 030.

[59] J. Bernabeu, A. Santamaria, J. Vidal, A. Mendez, and J. W. F. Valle, Lepton flavor nonconservation at high-energies in a superstring inspired standard model, Phys. Lett. B **187**, 303 (1987).

[60] M. Gonzalez-Garcia and J. W. F. Valle, Fast decaying neutrinos and observable flavor violation in a new class of Majoron models, Phys. Lett. B **216**, 360 (1989).

[61] A. Abada, M. E. Krauss, W. Porod, F. Staub, A. Vicente, and C. Weiland, Lepton flavor violation in low-scale seesaw models: SUSY and non-SUSY contributions, J. High Energy Phys. 11 (2014) 048.

[62] C. Hagedorn, J. Kriewald, J. Orloff, and A. M. Teixeira, Flavour and CP symmetries in the inverse seesaw, Eur. Phys. J. C **82**, 194 (2022).

[63] M. Dittmar, A. Santamaria, M. Gonzalez-Garcia, and J. W. F. Valle, Production mechanisms and signatures of isosinglet neutral heavy leptons in $Z^0$ decays, Nucl. Phys. **B332**, 1 (1990).

[64] M. Gonzalez-Garcia, A. Santamaria, and J. W. F. Valle, Isosinglet neutral heavy lepton production in $Z$ decays and neutrino mass, Nucl. Phys. **B342**, 108 (1990).

[65] A. Atre, T. Han, S. Pascoli, and B. Zhang, The search for heavy Majorana neutrinos, J. High Energy Phys. 05 (2009) 030.

[66] J. Aguilar-Saavedra, F. Deppisch, O. Kittel, and J. W. F. Valle, Flavour in heavy neutrino searches at the LHC, Phys. Rev. D **85**, 091301 (2012).

[67] S. Das, F. Deppisch, O. Kittel, and J. W. F. Valle, Heavy neutrinos and lepton flavour violation in left-right symmetric models at the LHC, Phys. Rev. D **86**, 055006 (2012).

[68] F. F. Deppisch, N. Desai, and J. W. F. Valle, Is charged lepton flavor violation a high energy phenomenon?, Phys. Rev. D **89**, 051302 (2014).

[69] S. Antusch and O. Fischer, Testing sterile neutrino extensions of the standard model at future lepton colliders, J. High Energy Phys. 05 (2015) 053.

[70] F. F. Deppisch, P. S. Bhupal Dev, and A. Pilaftsis, Neutrinos and collider physics, New J. Phys. **17**, 075019 (2015).

[71] M. Hirsch and Z. S. Wang, Heavy neutral leptons at ANUBIS, Phys. Rev. D **101**, 055034 (2020).

[72] G. Cottin, J. C. Helo, M. Hirsch, C. Peña, C. Wang, and S. Xie, Long-lived heavy neutral leptons with a displaced shower signature at CMS, J. High Energy Phys. 02 (2023) 011.

[73] G. Chauhan, P. S. B. Dev, I. Dubovyk, B. Dziewit, W. Flieger, K. Grzanka, J. Gluza, B. Karmakar, and S. Zieba, Phenomenology of lepton masses and mixing with discrete flavor symmetries, arXiv:2310.20681.

[74] A. Batra, P. Bharadwaj, S. Mandal, R. Srivastava, and J. W. F. Valle, Phenomenology of the simplest linear seesaw mechanism, J. High Energy Phys. 07 (2023) 221.

[75] S. Alekhin *et al.*, A facility to search for hidden particles at the CERN SPS: The SHiP physics case, Rep. Prog. Phys. **79**, 124201 (2016).

[76] CMS Collaboration, Search for heavy Majorana neutrinos in the same-sign dilepton channel in proton-proton collisions at $\sqrt{s} = 13$ TeV, arXiv:1806.10905.

[77] M. Aaboud *et al.* (ATLAS Collaboration), Search for heavy Majorana or Dirac neutrinos and right-handed $W$ gauge bosons in final states with two charged leptons and two jets at $\sqrt{s} = 13$ TeV with the ATLAS detector, J. High Energy Phys. 01 (2019) 016.

[78] J. Alimena *et al.*, Searching for long-lived particles beyond the standard model at the Large Hadron Collider, J. Phys. G **47**, 090501 (2020).

[79] A. Tumasyan *et al.* (CMS Collaboration), Search for long-lived heavy neutral leptons with displaced vertices in proton-proton collisions at $\sqrt{s} = 13$ TeV, J. High Energy Phys. 07 (2022) 081.

[80] A. M. Abdullahi *et al.*, The present and future status of heavy neutral leptons, J. Phys. G **50**, 020501 (2023).

[81] CMS Collaboration, Search for long-lived heavy neutral leptons with lepton flavour conserving or violating decays to a jet and a charged lepton, J. High Energy Phys. 03 (2024) 105.